Pilot-subcarrier Based Impulsive Noise Mitigation for Underwater Acoustic OFDM Systems

Peng Chen
Dept ECE
Curtin University
peng.ch@outlook.com

Yue Rong
Dept ECE
Curtin University
y.rong@curtin.edu.au

Sven Nordholm
Dept ECE
Curtin University
s.nordholm@curtin.edu.au

ABSTRACT

Orthogonal frequency-division multiplexing (OFDM) technique has become a popular choice for underwater acoustic (UA) networks recently. Impulsive noise is one of the factors that limit the performance of this technique, and the mitigation of impulsive noise receives increasing attention in the UA communication community. In this paper, a pilot-based algorithm is proposed to mitigate the impact of impulsive noise. The proposed algorithm introduces a special OFDM block as preamble during which impulsive noise mitigation is performed using the null subcarriers and then the channel response is estimated using pilot subcarriers. By assuming that the channel is quasi-stationary, the proposed algorithm adopts the channel estimation result of the previous block to estimate and mitigate the impulsive noise of the current block. We apply the proposed algorithm to process the data collected during the experiment conducted in December 2015, in the estuary of the Swan River, Western Australia. The results show that the proposed approach is able to mitigate the impulsive noise for UA OFDM systems.

Keywords

Underwater communication, channel estimation, impulsive noise

1. INTRODUCTION

The underwater acoustic (UA) channel is one of the most challenging channels for wireless communication mainly because of the rapid dispersion in both time and frequency domains [1]. Moreover, UA communication is also impacted by impulsive noise which is introduced by natural sources and/or human activities [2], [3].

Orthogonal frequency-division multiplexing (OFDM) systems have become a popular choice for UA communication during recent years due to their strong capability in mitigating rapid frequency dispersions [4]-[6]. This type of systems are, however, significantly impacted by impulsive noise [7], [8]. One popular method to mitigate impulsive noise for these systems is to detect the samples affected by impulsive noise using threshold testing and then adjust those samples using blanking or clipping techniques in the time domain [7]. Another popular method is to use null subcarriers to estimate the impulsive noise samples utilizing the sparsity of the impulsive noise [9]. We would like to note that the first method fails to exploit the OFDM signal structure while the second method requires extra bandwidth for null subcarriers.

In this paper, we propose a pilot-subcarrier based impulsive noise mitigation algorithm for frame-based UA OFDM communications. During the preamble of each frame, the proposed algorithm utilizes the null subcarriers to mitigate the effect of impulsive noise and then exploits the received pilot subcarriers to perform channel estimation. During each data block, the proposed algorithm uses the estimated channel impulse response of the previous block to mitigate the impulsive noise of the current block.

We apply the proposed algorithm to process the data collected during the experiment conducted in December 2015, in the estuary of the Swan River, Western Australia. The results show that compared with the blanking method, the proposed algorithm reduces the system bit-error-rate (BER) due to an improved performance in mitigating the impulsive noise.

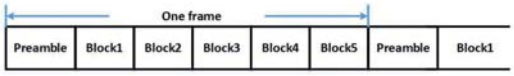

Figure 1: Frame structure of the transmitted signals.

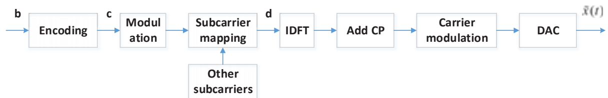

Figure 2: Block diagram of the transmitter in a UA OFDM communication system.

2. SYSTEM MODEL

In this paper, we consider a frame-based coded UA OFDM communication system. The frame structure of the transmitted signals is shown in Fig. 1. A special OFDM block is introduced as preamble for the purpose of synchronization and initial channel estimation. This preamble block has N_c

WUWNET '16, October 24-26, 2016, Shanghai, China

DOI: http://dx.doi.org/10.1145/2999504.3001106

subcarriers, half of which are used for pilots and the other half are blank. Both the pilot subcarriers and the null subcarriers are equally spaced. Let us introduce $\mathcal{I}_n$ as a set containing the positions (indices) of null subcarriers among N_c subcarriers.

For data blocks, Fig. 2 shows the transmitter structure. In each frame, a binary source data stream $\boldsymbol{b} = (b[1], \ldots, b[L_b])^T$ is encoded, interleaved, and punctured to form a coded sequence $\boldsymbol{c} = (c[1], \ldots, c[L_c])^T$ with length $L_c = R_m N_s N_b$, where $(\cdot)^T$ denotes the matrix (vector) transpose, L_b is the number of information-carrying bits in each frame, R_m denotes the modulation order, N_s is the number of data subcarriers, and N_b denotes the number of OFDM blocks in one frame. Note that as the algorithm to be presented is independent of the channel coding scheme, any code (such as the turbo code and the convolutional code) can be used. The coded sequence $\boldsymbol{c}$ is mapped into $N_s N_b$ data symbols taken from the phase-shift keying (PSK) or quadrature amplitude modulation (QAM) constellations. Then every N_s data symbols together with N_p quadrature PSK (QPSK) modulated pilot symbols are mapped into one OFDM symbol vector $\boldsymbol{d} = (d[1], \ldots, d[N_c])^T$, where N_p is the number of pilot subcarriers. We denote $\mathcal{I}_p$ as the indices of subcarriers with pilot symbols. We assume that pilot subcarriers are uniformly spaced and denote $\boldsymbol{d}_p$ as the pilot sequence in one OFDM block.

Passband signals are directly generated for each OFDM block at the transmitter. Let f_{sc} denote the subcarrier spacing. The bandwidth of the transmitted signal is $B = f_{sc} N_c$ and the duration of one OFDM symbol is $T = 1/f_{sc}$. The N_c subcarriers are located at frequencies of

$$f_k = f_c + k f_{sc}, \quad k = -\frac{N_c}{2} + 1, \ldots, \frac{N_c}{2}$$

where f_c is the center carrier frequency. To enable simple one-tap equalization and to avoid interference among OFDM blocks, a cyclic prefix (CP) of length T_{cp} is prepended to the OFDM symbol, and the total length of one OFDM block is $T_{total} = T + T_{cp}$. The continuous time representation of an OFDM block can be expressed as

$$\begin{aligned} \tilde{x}(t) &= 2\mathrm{Re}\left\{ \left[\frac{1}{\sqrt{N_c}} \sum_{k=-\frac{N_c}{2}+1}^{\frac{N_c}{2}} \check{d}[k] e^{j2\pi k f_{sc} t} \right] e^{j2\pi f_c t} \right\}, \\ &\qquad\qquad 0 \le t \le T \\ \tilde{x}(t) &= \tilde{x}(t+T), \qquad -T_{cp} \le t < 0 \end{aligned} \tag{1}$$

where $\mathrm{Re}\{\cdot\}$ denotes the real part of a complex number and

$$\check{d}[k] = \begin{cases} d[k], & 1 \le k \le \frac{N_c}{2} \\ d[k+N_c], & -\frac{N_c}{2} + 1 \le k \le 0 \end{cases}.$$

During each block, a stationary UA channel with L_p paths can be represented as

$$h(t) = \sum_{l=1}^{L_p} A_l \delta(t - \tau_l) \tag{2}$$

where A_l and τ_l denote the amplitude and delay of the lth path, respectively. We also assume that the channel is quasi-stationary between two adjacent data blocks.

Then the received passband signal of one OFDM block is given by

$$\tilde{r}(t) = 2\mathrm{Re}\left\{ \sum_{l=1}^{L_p} A_l \tilde{x}(t - \tau_l) \right\} + \tilde{v}(t) + \tilde{w}(t) \tag{3}$$

where $\tilde{v}(t)$ is the passband impulsive noise and $\tilde{w}(t)$ represents other non-impulsive background noise. After removing the CP, downshifting, and low-pass filtering $\tilde{r}(t)$, the baseband received signal can be obtained from (1) and (3) as

$$\begin{aligned} r(t) &= \sum_{l=1}^{L_p} \frac{A_l e^{-j2\pi f_c \tau_l}}{\sqrt{N_c}} \sum_{k=-\frac{N_c}{2}+1}^{\frac{N_c}{2}} \check{d}[k] e^{j2\pi k f_{sc}(t-\tau_l)} + v(t) + w(t) \\ &= \frac{1}{\sqrt{N_c}} \sum_{k=-\frac{N_c}{2}+1}^{\frac{N_c}{2}} \check{d}[k] e^{j2\pi k f_{sc} t} \sum_{l=1}^{L_p} A_l e^{-j2\pi f_k \tau_l} \\ &\quad + v(t) + w(t), \qquad 0 \le t \le T \end{aligned} \tag{4}$$

where $v(t)$ and $w(t)$ are the baseband impulsive noise and other noise, respectively. From (4), the channel frequency response at the kth subcarrier is given by

$$H[k] = \sum_{l=1}^{L_p} A_l e^{-j2\pi f_k \tau_l}, \quad k = -\frac{N_c}{2} + 1, \ldots, \frac{N_c}{2}.$$

By sampling $r(t)$ at the rate of $1/B$, we obtain discrete time samples of one OFDM symbol from (4) as

$$\begin{aligned} r[i] &= \frac{1}{\sqrt{N_c}} \sum_{k=-\frac{N_c}{2}+1}^{\frac{N_c}{2}} \check{d}[k] e^{j2\pi i k f_{sc}/B} H[k] + v[i] + w[i] \\ &= \frac{1}{\sqrt{N_c}} \sum_{k=-\frac{N_c}{2}+1}^{\frac{N_c}{2}} \check{d}[k] e^{j2\pi i k / N_c} H[k] + v[i] + w[i], \\ &\qquad\qquad i = 1, \ldots, N_c \end{aligned} \tag{5}$$

where $v[i]$ is the impulsive noise samples and $w[i]$ is zero-mean additive Gaussian noise samples, respectively. The matrix-vector form of (5) is given by

$$\begin{aligned} \boldsymbol{r} &= \boldsymbol{F}^H \boldsymbol{D} \boldsymbol{h}_f + \boldsymbol{v} + \boldsymbol{w} \\ &= \boldsymbol{F}^H \boldsymbol{D} \boldsymbol{F} \boldsymbol{h}_t + \boldsymbol{v} + \boldsymbol{w} \end{aligned} \tag{6}$$

where $\boldsymbol{D} = \mathrm{diag}(\boldsymbol{d})$ is a diagonal matrix taking $\boldsymbol{d}$ as the main diagonal elements, $(\cdot)^H$ denotes the conjugate transpose, $\boldsymbol{F}$ is an $N_c \times N_c$ discrete Fourier transform (DFT) matrix with the (i,k)-th entry of $1/\sqrt{N_c} e^{-j2\pi(i-1)(k-1)/N_c}$, $i, k = 1, \ldots, N_c$, $\boldsymbol{r} = (r[1], \ldots, r[N_c])^T$, $\boldsymbol{v} = (v[1], \ldots, v[N_c])^T$, $\boldsymbol{w} = (w[1], \ldots, w[N_c])^T$. In (6), $\boldsymbol{h}_f = (h_f[1], \ldots, h_f[N_c])^T$ is a vector containing the channel frequency response at all N_c subcarriers with

$$h_f[k] = \begin{cases} H[k], & 1 \le k \le \frac{N_c}{2} \\ H[k - N_c], & \frac{N_c}{2} + 1 \le k \le N_c \end{cases}$$

and $\boldsymbol{h}_t = \boldsymbol{F}^H \boldsymbol{h}_f$ is the discrete time domain representation of the channel impulse response with a maximum delay of $L_m = \lceil B \tau_{L_p} \rceil$.

From (6), the frequency domain representation of the re-

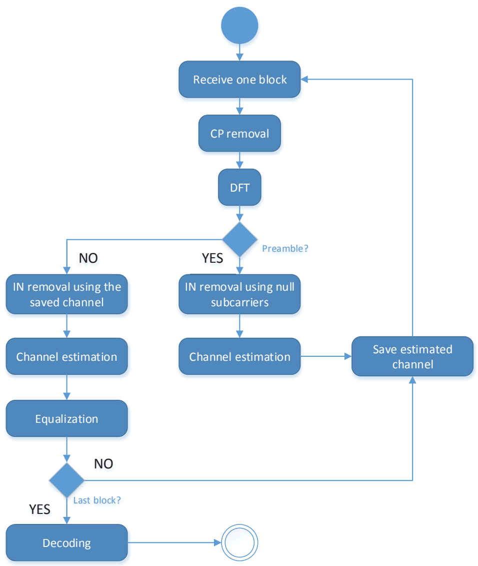

Figure 3: Baseband signal processing at the receiver using the proposed algorithm.

ceived signal can be written as

$$\begin{aligned} \boldsymbol{r}_f &= \boldsymbol{F}\boldsymbol{r} \\ &= \boldsymbol{F}\boldsymbol{F}^H\boldsymbol{D}\boldsymbol{h}_f + \boldsymbol{F}\boldsymbol{v} + \boldsymbol{F}\boldsymbol{w} \\ &= \boldsymbol{D}\boldsymbol{h}_f + \boldsymbol{v}_f + \boldsymbol{w}_f \end{aligned} \tag{7}$$

where $\boldsymbol{v}_f = \boldsymbol{F}\boldsymbol{v}$ and $\boldsymbol{w}_f = \boldsymbol{F}\boldsymbol{w}$ are the impulsive noise and other noise in the frequency domain, respectively.

3. PROPOSED ALGORITHM

The baseband signal processing at the receiver using the proposed algorithm is shown in Fig. 3. As the received signals are contaminated by impulsive noise, for both the data blocks and preambles, the receiver estimates and removes the impulsive noise before performing channel estimation. In particular, after receiving an OFDM block and removing the CP, the receiver checks whether the current block is a preamble block or a data block, based on which different procedures are taken. For preamble blocks, the IN removal process is performed by using the null subcarriers, and then the receiver estimates and saves the current channel response. For data blocks, the receiver estimates and removes the IN by using pilot subcarriers and the channel response of the previous block, and then performs channel estimation and equalization. If the current block is not the last block of the frame, the receiver saves the estimated channel response and starts processing the next block. Otherwise, the receiver starts decoding the source data $\boldsymbol{b}$ in this frame.

3.1 Impulsive Noise Position Detection

To estimate the impulsive noise, the receiver needs to find the samples affected by impulsive noise using a thresholding method. For each block the receiver firstly finds the average energy G of the current OFDM block and then collects the positions of samples possibly contaminated by impulsive noise into a vector $\mathcal{I}_I$ which satisfies

$$|r[\mathcal{I}_I[i]]|^2 > G\beta$$

for $i = 1, \ldots, N_I$, where β is a relative threshold and N_I is the number of possible positions. Let us introduce an $N_c \times N_I$ position selection matrix for each block

$$\boldsymbol{P}_I[i,k] = \begin{cases} 1, & i = \mathcal{I}_I[k] \\ 0, & \text{otherwise} \end{cases}.$$

3.2 Impulsive Noise Estimation During the Preamble Block

Let us define $\boldsymbol{P}_n$ as an $N_c/2 \times N_c$ matrix with unit entries at the $(i, \mathcal{I}_n[i])$-th position, $i = 1, \ldots, N_c/2$, the signals received at the null subcarriers of the preamble can be expressed as

$$\begin{aligned} \boldsymbol{r}_n &= \boldsymbol{P}_n\boldsymbol{r}_f \\ &= \boldsymbol{P}_n\boldsymbol{F}\boldsymbol{v} + \boldsymbol{P}_n\boldsymbol{w}_f \\ &= \boldsymbol{P}_n\boldsymbol{F}\boldsymbol{P}_I\boldsymbol{v}_I + \boldsymbol{w}_n \end{aligned} \tag{8}$$

where $\boldsymbol{v}_I$ is a vector containing all the N_I samples of the impulsive noise during the preamble and $\boldsymbol{w}_n = \boldsymbol{P}_n\boldsymbol{w}_f$. By introducing

$$\boldsymbol{F}_{I,p} = \boldsymbol{P}_n\boldsymbol{F}\boldsymbol{P}_I \tag{9}$$

we can estimate the impulsive noise using the least-squares (LS) approach as

$$\hat{\boldsymbol{v}}_I = (\boldsymbol{F}_{I,p}^H\boldsymbol{F}_{I,p})^{-1}\boldsymbol{F}_{I,p}^H\boldsymbol{r}_n \tag{10}$$

where $(\cdot)^{-1}$ denotes matrix inversion. Finally, the receiver maps $\hat{\boldsymbol{v}}_I$ into an N_c-elements vector $\hat{\boldsymbol{v}}$ using $\boldsymbol{P}_I$ to reconstruct the impulsive noise as

$$\hat{\boldsymbol{v}} = \boldsymbol{P}_I\hat{\boldsymbol{v}}_I \tag{11}$$

and removes the impulsive noise from the received preamble by

$$\check{\boldsymbol{r}}_f = \boldsymbol{r}_f - \boldsymbol{F}\hat{\boldsymbol{v}}. \tag{12}$$

Then the receiver uses the pilot subcarriers of $\check{\boldsymbol{r}}_f$ to perform channel estimation.

3.3 Pilot-subcarrier Based Impulsive Noise Estimation During Data Blocks

Based on the assumption that the UA channel is quasi-stationary within one frame, we propose to estimate the impulsive noise samples of the current block by exploiting the signals received at the pilot subcarriers and the channel impulse response estimated from the previous block. Defining $\boldsymbol{P}$ as an $N_p \times N_c$ matrix with unit entries at the $(i, \mathcal{I}_p[i])$-th position, $i = 1, \ldots, N_p$, the signal vector received at the pilot subcarriers of the current data block is given by

$$\begin{aligned} \boldsymbol{r}_p &= \boldsymbol{P}\boldsymbol{r}_f \\ &= \boldsymbol{D}_p\boldsymbol{P}\boldsymbol{h}_f + \boldsymbol{P}\boldsymbol{F}\boldsymbol{v} + \boldsymbol{P}\boldsymbol{w}_f \\ &= \boldsymbol{D}_p\boldsymbol{P}\check{\boldsymbol{h}}_f + \boldsymbol{D}_p\boldsymbol{P}(\boldsymbol{h}_f - \check{\boldsymbol{h}}_f) + \boldsymbol{P}\boldsymbol{F}\boldsymbol{v} + \boldsymbol{P}\boldsymbol{w}_f \\ &= \boldsymbol{D}_p\boldsymbol{P}\check{\boldsymbol{h}}_f + \check{\boldsymbol{w}}_p + \boldsymbol{P}\boldsymbol{F}\boldsymbol{v} \end{aligned} \tag{13}$$

where $\boldsymbol{D}_p = \text{diag}(\boldsymbol{d}_p)$, $\check{\boldsymbol{w}}_p = \boldsymbol{D}_p\boldsymbol{P}(\boldsymbol{h}_f - \check{\boldsymbol{h}}_f) + \boldsymbol{P}\boldsymbol{w}_f$, and $\check{\boldsymbol{h}}_f$ is the channel frequency response estimated at the previous block. Due to the assumption of quasi-stationary channel, we have $\boldsymbol{h}_f \approx \check{\boldsymbol{h}}_f$.

Introducing $\boldsymbol{v}_I$ as a vector containing all the N_I samples of impulsive noise in the current OFDM block, we rewrite the impulsive noises as

$$\boldsymbol{v} = \boldsymbol{P}_I\boldsymbol{v}_I. \tag{14}$$

Figure 4: Transmitter and receiver locations during the experiment.

By substituting (14) back into (13), the impulsive noise can be estimated using the LS method as:

$$\hat{\boldsymbol{v}}_I = (\boldsymbol{F}_{I,d}^H \boldsymbol{F}_{I,d})^{-1} \boldsymbol{F}_{I,d}^H (\boldsymbol{P}\boldsymbol{r}_f - \boldsymbol{D}_p \boldsymbol{P} \breve{\boldsymbol{h}}_f) \tag{15}$$

where $\boldsymbol{F}_{I,d} = \boldsymbol{P}\boldsymbol{F}\boldsymbol{P}_I$. The receiver maps $\hat{\boldsymbol{v}}_I$ into an N_c-elements vector $\hat{\boldsymbol{v}}$ using (14) to reconstruct the impulsive noise and finally subtracts $\hat{\boldsymbol{v}}$ from the received signal $\boldsymbol{r}$ using (12) and the resulting signals are passed to channel equalization and decoding operations.

4. EXPERIMENT ARRANGEMENT

The locations of the transmitter and receiver during the experiment are shown in Fig. 4, where the distance between the transmitter and receiver was 936 meters. The water depth along the direct path varied between 2.5 and 6 meters, which was very shallow. Both the transmitter transducer and the receiver hydrophone were attached through cables to steel frames a half meter above the river bed. The water depths at the transmitter and the receiver were 5 meters and 2.5 meters, respectively. The movement of the hydrophone and the transducer was small as they were attached to steel frames. As the hydrophone was located in warm shallow water close to a jetty, there was a significant amount of highly impulsive snapping shrimp noise. Another source of impulsive noise during the experiment was from waves breaking at the jetty piers whose intensity increases with the wind speed. To investigate the impact of wind on the breaking wave noise, the same data file was transmitted three times during the day under different wind conditions.

Key parameters for both the preamble blocks and the data blocks of the experimental system are summarized in Table 1. As shown in Fig. 1, each frame contains 5 OFDM data blocks and one preamble block. Among the total 512 subcarriers, there are 325 data subcarriers, 128 uniformly spaced pilot subcarriers for channel estimation, 18 null subcarriers at each edge of the passband, and 23 subcarriers for frequency offset estimation. The pilot symbols are modulated by QPSK constellations. The data symbols are modulated by QPSK constellations encoded by either 1/2 or 1/3 rate turbo codes. Considering the code puncturing, the number of information-carrying bits in each frame is $L_b = 1632$ (1/2 rate), $L_b = 1088$ (1/3 rate). Thus, the system source data rate is

$$R_b = \frac{L_b}{(T+T_{cp})(N_b+1)} = \begin{cases} 1.19 \text{ kb/s}, & 1/3 \text{ rate} \\ 1.78 \text{ kb/s}, & 1/2 \text{ rate} \end{cases}.$$

Each transmission contains 500 frames with 250 frames for every coding rate. The data files recorded at the receiver during three transmissions were named T83, T84, and T85, respectively.

Table 1: Experimental System Parameters.

Number of OFDM blocks	N_b	5
Bandwidth	B	4 kHz
Carrier frequency	f_c	12 kHz
Sampling rate	f_s	96 kHz
Number of subcarriers	N_c	512
Subcarrier spacing	f_{sc}	7.8 Hz
Length of OFDM symbol	T	128 ms
Length of CP	T_{cp}	25 ms

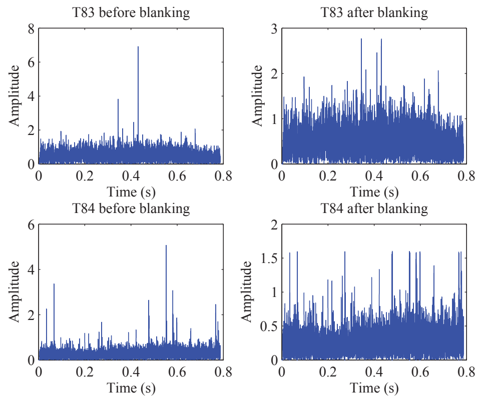

Figure 5: Amplitude of the received signals in a typical frame of the T83 and the T84 files.

5. EXPERIMENT RESULTS

In the experimental system, symbol synchronization was achieved by performing cross-correlation between the received preamble and the local version. This synchronization algorithm worked perfectly for the T83 and T85 files, but failed to find the head of 4 and 2 data frames for the 1/3 rate and 1/2 rate signals, respectively, in the T84 file, due to the dense impulsive noise. In fact, among the three recorded data files, the T84 file contains signals most heavily affected by the impulsive noise, while signals in the T83 file are least impacted by the impulsive noise. The amplitude of the received signals in a typical data frame taken from the T83 and the T84 files is shown in Fig. 5. It can be seen that even after the blanking operation, there is still a significant amount of impulsive noise in the T84 file.

As the transmitter and receiver were attached to fixed steel frames, the channel Doppler shift was small during the experiment. Fig. 6 shows the Doppler shift estimated by the preamble block in each frame of the T83 file. It can be seen that as the Doppler shift of most of the frames is smaller than 0.2 Hz, the step of Doppler shift compensation can be skipped when processing the received data.

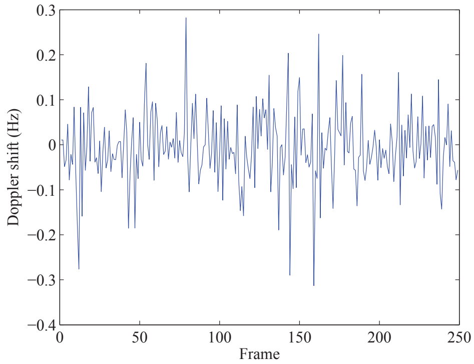

Figure 6: Doppler shift estimated by the preamble blocks in the T83 file.

Table 2: Performance Comparison for the T83 File.

Rate	Method	Raw BER	Coded BER	FER
1/3	LS w/o Blanking	6.2%	0.2%	0.4%
	LS + Blanking	5.2%	0	0
	Proposed	4.0%	0	0
1/2	LS w/o Blanking	5.6%	0.3%	1.6%
	LS + Blanking	4.7%	0	0
	Proposed	3.6%	0	0

We compare the system performance yielded by the blanking method and the proposed algorithm. For impulsive noise position detection, we set the threshold $\beta = 5$ which maximizes the performance of the blanking algorithm. The system BER and frame error rate (FER) are shown in Tables 2-4 for the three files, respectively. We adopt the soft decoding algorithm for the turbo decoding process, so both the raw BER and the coded BER reflect the advantage of the proposed algorithm. To calculate the FER, one frame is considered erroneous if one or more of the L_b information-carrying bits in this frame is incorrectly decoded.

The results show that both the blanking method and the proposed algorithm are able to improve the receiver performance while the proposed algorithm leads to lower system BER and FER. Compared with the blanking method, the proposed algorithm decreases the raw BER by around 1% for all the three files. The proposed algorithm also significantly reduces the coded BER of the 1/2 rate signal of the T84 file by about 9%, and the FER by about 9% for 1/2 rate signals of both the T84 and T85 files.

6. CONCLUSIONS

In this paper, a new algorithm has been proposed to mitigate the impact of impulsive noise in UA OFDM systems by using pilots subcarriers. The proposed algorithm introduces a special preamble where the impulsive noise is estimated by using the null subcarriers and an initial channel estimation is obtained by using the pilot subcarriers. By assuming that the channel is quasi-stationary, we use the estimated channel from the previous block to estimate the impulsive noise of the current block. Field experiments were conducted and it is shown that the proposed algorithm outperforms the blanking method.

Table 3: Performance Comparison for the T84 File.

Rate	Method	Raw BER	Coded BER	FER
1/3	LS w/o Blanking	18.7%	10.9%	50.4%
	LS + Blanking	15.5%	1.3%	7.3%
	Proposed	14.8%	1.0%	6.1%
1/2	LS w/o Blanking	18.1%	22.5%	93.6%
	LS + Blanking	14.6%	15.9%	84.7%
	Proposed	14.1%	6.9%	75.8%

Table 4: Performance Comparison for the T85 File.

Rate	Method	Raw BER	Coded BER	FER
1/3	LS w/o Blanking	13.5%	1.6%	6.4%
	LS + Blanking	11.2%	0	0
	Proposed	10.0%	0	0
1/2	LS w/o Blanking	15.0%	15.3%	71.6%
	LS + Blanking	11.7%	3.9%	24.8%
	Proposed	11.0%	1.1%	15.2%

Acknowledgment

This research was supported under the Australian Research Council's Discovery Projects funding scheme (project number DP140102131).

7. REFERENCES

[1] M. Stojanovic and J. Preisig. Underwater acoustic communication channels: Propagation models and statistical characterization. *IEEE Commun. Magazine*, 47(1):84–89, January 2009.

[2] J. Hildebrand. Anthropogenic and natural sources of ambient noise in the ocean. *Marine Ecology Progress Series*, 395:5–20, December 2009.

[3] M. Chitre, S. Kuselan, and V. Pallayil. Ambient noise imaging in warm shallow waters; robust statistical algorithms and range estimation. *J. Acoustical Society of America*, 132(2):838–847, August 2012.

[4] Z. Wang, S. Zhou, J. Catipovic, and P. Willett. Asynchronous multiuser reception for OFDM in underwater acoustic communications. *IEEE Trans. Wireless Commun.*, 12(3):1050–1061, March 2013.

[5] B. Li, S. Zhou, M. Stojanovic, L. L. Freitag, and P. Willett. Multicarrier communication over underwater acoustic channels with nonuniform Doppler shifts. *IEEE J. Ocean. Eng.*, 33(2):1638–1649, April 2008.

[6] H. Yan, L. Wan, S. Zhou, Z. Shi, J. H. Cui, J. Huang, and H. Zhou. DSP based receiver implementation for OFDM acoustic modems. *J. Phys. Commun.*, 5(1):22–32, March 2012.

[7] T. Suzuki, H. M. Tran, and T. Wada. An underwater acoustic OFDM communication system with shrimp (impulsive) noise cancelling. *Int. Conf. Computing, Management and Telecommunications*, pages 152–156. April 2014.

[8] M. Chitre, S. H. Ong, and J. Potter. Performance of coded OFDM in very shallow water channels and snapping shrimp noise. In *Proc. MTS/IEEE OCEANS*, pages 996–1001. September 2005,.

[9] H. Sun, W. Shen, Z. Wang, S. Zhou, X. Xu, and Y. Chen. Joint carrier frequency offset and impulse noise estimation for underwater acoustic OFDM with null subcarriers. In *Proc. MTS/IEEE OCEANS*, pages 1–4. October 2012.